PHYSICAL REVIEW B **75**, 220403(R) (2007)

Spin-transfer-torque-driven domin-wall dynamics in Permalloy nanowires

Shuqiang Yang and J. L. Erskine
Department of Physics, The University of Texas at Austin, Austin, Texas 78712, USA
(Received 10 July 2006; revised manuscript received 19 May 2007; published 13 June 2007)

Pulse-current-driven domain-wall (DW) dynamics in Permalloy nanowires are studied using high-temporal-resolution magneto-optical techniques. The time-resolved measurements reveal prompt displacements proportional to current density above a well-defined threshold and yield values of DW velocity and spin-flip efficiency that are a factor of 10 higher than those determined in prior experiments. A stochastic variation in the wall displacements associated with termination of the current pulse is observed. The experimental results suggest the presence of both adiabatic and nonadiabatic spin-transfer-torque mechanisms, but do not appear to be fully explained by existing theoretical models.

DOI: 10.1103/PhysRevB.75.220403 PACS number(s): 75.60.Ch, 75.75.+a

Manipulation of spin distributions on a submicron scale plays a central role in data storage devices and also offers new opportunities for future electronics technology[1–3] termed "spintronics." Recent theoretical[4–10] and experimental[11–15] work has addressed the underlying physical basis of magnetic domain-wall (DW) manipulation by electric current. While these studies have advanced the understanding of current-driven DW phenomena beyond the pioneering work of Berger[16–18] and others, striking discrepancies remain between experiments and corresponding results obtained from existing phenomenological models and numerical simulations.

Specific discrepancies can be found in studies of pulsed electric-current-driven DW motion in thin-film-based Permalloy nanowires. The nanowire structures are small enough to permit numerical simulation of DW dynamics based on solving the modified Landau-Lifschitz-Gilbert (LLG) equation.[5–9] These model (one-dimensional) systems are ideal for exploring both magnetic-field-[3,19,20] and electric-current-[11–14] driven DW dynamics.

Recent experiments on field-only-driven DW dynamics[20] have yielded results in essential agreement with phenomenological descriptions and numerical simulations.[21] To account for the effects of electric current, two terms have been added to the LLG equation,[6] which correspond to "adiabatic"[4–9] and "nonadiabatic"[4,6,13,17] spin-transfer torques. The spin-transfer-torque mechanism, which drives DW distortion and propagation, is described by a velocity parameter,[5,8] $b_j = Pj\mu_B/(eM_s)$ and a spin-flip efficiency parameter $\epsilon = v/b_j$ that is equivalent to the ratio of displaced DW spins flipped per polarized conduction electron. The symbols correspond to j=current density, μ_B=Bohr magneton, e=electronic charge, and v=DW velocity; and for Permalloy, typical parameters for the conduction electron polarization P and saturation magnetization M_s are, respectively, 0.5 and 8.0×10^5 A/m^2. Theoretical models[6–8] of adiabatic current-driven DW displacements and velocities in Permalloy nanowire structures (assuming Gilbert damping) at $j=10\times10^{12}$ A/m^2 (below $j_{cr}\sim10^{14}$ A/m^2, the theoretical threshold for sustained motion) predict initial velocities $v_{max}=400$ m/s that decay to about 100 m/s after 0.5 ns (and essentially to zero after 2 ns), with corresponding total displacements of $\Delta x\cong150$ nm. Under these conditions, the maximum spin-flip efficiency (which occurs at $t=0$ when the current step is applied) is $\epsilon_{max}=eM_s/P\mu_B(v_{max}/j)=2.76\times10^{10}(v_{max}/j)\approx1$, a value consistent with the assumption that conduction electron spins follow the local magnetization within the DW and transfer all of their spin momentum to the displaced wall. Analytical models of adiabatic current-driven DW motion[4] appear to be generally consistent with the results of LLG simulations summarized above. A recent theoretical analysis[22] of spin-transfer-driven DW dynamics that assumes Landau-Lifschitz damping predicts qualitatively different time-dependent displacements: sustained motion characterized by b_j.

Recent experiments[23,24] that explore dc-current-driven enhancement of field-driven DW motion in Permalloy nanowires verify the existence of a steady-state current-driven force in the presence of an applied magnetic field. The velocity enhancements ($v\sim35$ m/s at $j=6\times10^{11}$ A/m^2) and corresponding high values of spin-flip efficiency ($\epsilon\sim0.7$) are comparable with terminal velocities estimated from nonadiabatic corrections[6] to the adiabatic term in the LLG equations. The corresponding situation for pulse-current-driven DW displacements in Permalloy nanowires in the absence of an applied magnetic field is less clear.

Existing experimental estimates of current-driven DW velocities and spin-flip efficiencies have been based primarily on observation of pulse-driven DW displacements Δx using magnetic force microscopy (MFM).[11,12] Temporal resolution is achieved by using short-duration pulses to drive the DW and the (average) wall velocity is calculated by assuming that $v=\Delta x/$(pulse duration). The experiments have yielded estimates of prompt current-driven DW velocities in Permalloy nanowires ranging from 0.4 to 4 m/s and spin-flip efficiencies of $\epsilon<0.1$ at current densities of $\sim7\times10^{11}$ A/m^2 using pulse durations of 0.3–5.0 μs. These values of v and ϵ are at least a factor of 10 lower than theoretical estimates.[5,8,9] The discrepancies have been attributed to dissipation of spin-polarized-current angular momentum by spin-wave creation associated with DW depinning.[4] Additional features of selected experimental results are that the measured DW displacements are observed to be proportional to the pulse duration[11] and dependent on pulse rise time.[14] This behavior is inconsistent with the prompt dynamics based on the adiabatic spin-torque mechanism.[5,8,9] Some of the discrepancies

between experiments and (adiabatic term) theoretical predictions could be explained by nonadiabatic corrections to the spin-torque mechanism; however, recent evaluation of the spin-transfer-torque terms by Xiao, Zangwill, and Stiles[10] casts doubt on the existence of a significant nonadiabatic contribution to the torque term at zero field proposed by Zhang and Li.[6] We note other experiments[15] that report that the wall displacement does not depend on pulse duration and that most measurements[11,12,15] of pulse-current-driven DW displacements obtain values ($\Delta x \sim$ several μm) considerably larger than those predicted based on the adiabatic mechanism ($\Delta x \sim 100$ nm).[5,8] All of these results suggest the need for more precise measurements of pulse-current-driven DW phenomena with sufficiently high temporal resolution to reveal the DW dynamics, at least on a short time scale compared to the pulse duration.

The experiment reported in this paper overcomes some of the limitations of prior measurements of electric-current-driven DW displacement by using high-temporal-resolution magneto-optic Kerr effect (MOKE) tracking of the motion. While our experimental results do not appear fully compatible with existing models of current-driven DW motion, the results are interpreted within the framework of the adiabatic and nonadiabatic spin-transfer torque mechanisms. The experiments manifest DW displacements that are proportional to current density for $j > j_t$ (experimental threshold current required to depin the DW) and independent of pulse duration for pulses longer than the intrinsic time resolution of the experiment (0.3 μs). The experiments determine estimates of averaged current-driven DW velocities (as high as $v \geqslant 15$ m/s at $j = 4 \times 10^{11}$ A/m^2) and high spin-flip efficiencies ($\epsilon \sim 1$) that are consistent with the transient DW motion predicted theoretically for adiabatic-torque-driven wall motion. The factor-of-10 higher measured current-driven velocities and spin-flip efficiencies determined by our experiment show that pinning effects do not necessarily absorb most of the available spin angular momentum in current pulses having amplitude sufficiently above a threshold value.

Figure 1 illustrates essential features of the experiments. The 30-nm-thick, 500-nm-wide Permalloy ($Ni_{80}Fe_{20}$) microstructure was fabricated on an oxide-coated Si(100) wafer by e-beam lithography. Two orthogonal electromagnets allow application of B fields parallel to the orthogonal nanowire sections to prepare a stationary (vortex structure) (Refs. 25 and 26) DW within the field-of-view of the MOKE polarimeter. The high-speed MOKE polarimeter has been described previously[27] and used to study Barkhausen phenomena in thin-film Permalloy microstructures[28] and field-assisted current-driven DW dynamics.[23] The polarimeter utilizes a solid-state laser incident at 45° with s polarization focused on a 10-μm spot ($1/e$ width, major axis) at the wafer surface. The detected (longitudinal configuration) MOKE signal is proportional to the net magnetization $\langle M(x,t) \rangle$ of the microstructure (weighted by the beam intensity profile over the field of view). The polarimeter achieves temporal resolution of approximately 0.3 μs (preamplifier bandwidth-limited rise time), and the well-defined geometry of the experiment (including the feature that the DW width $\ll$ beam diameter) permits accurate time-resolved measurements of DW displacements. The sample temperature was determined by high temporal resolution measurements of the microstructure resistance ($R = 2.24$ kΩ at 300 K) using calibration data for Permalloy reported by Yamaguchi *et al.*[12] Figure 1 displays the current response to voltage step functions (rise time $t_r \sim 10$ ns) applied to a 2.24-kΩ carbon resistor and to the microstructure. The thermal relaxation time is approximately $\tau \approx 50$ ns. The sample temperature increases from 300 K to 630 K (in about 50 ns) at $j = 4 \times 10^{11}$ A/m^2 corresponding to a 25% reduction in M_s ($T_c = 820$ K for Permalloy).[29]

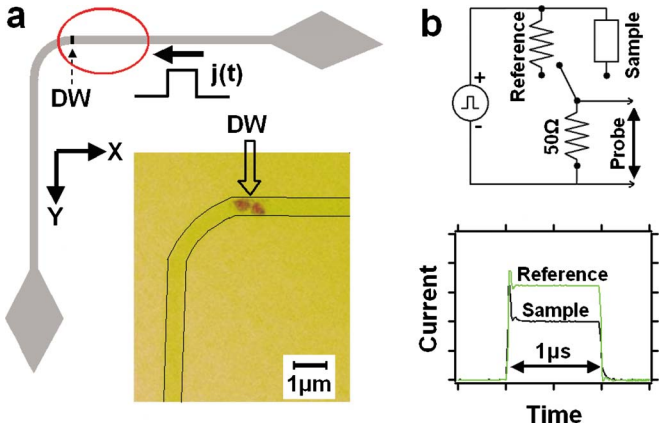

FIG. 1. (Color online) Panel (a): schematic of Permalloy microstructure. Ellipse enclosing a DW indicates $1/e$ intensity profile of focused laser beam. Inset: MFM image of the microstructure showing an injected vortex DW. Panel (b): pulse-current measurement (100 MHz sampling rate) of microstructure resistance $R(t)$ that establishes the temperature rise due to Ohmic heating.

Figure 2 displays a typical time-resolved measurement of electric-current-induced DW displacement for a pulse having $t_r \approx \tau$. Each point corresponds to a 0.1 μs sample of the magnetization $\langle M(x,t) \rangle$. Head-to-head or tail-to-tail DWs are prepared as shown in the MFM image (Fig. 1). The depinning field for a prepared DW is approximately 10 Oe. The prepared DW is then subjected (with $B = 0$) to an applied current pulse, resulting in a DW displacement in the direction of electron flow. The DW position within the MOKE polarimeter field of view is related to the detected MOKE intensity by an error function erf(x) due to the Gaussian laser beam profile.

Plots of the DW displacement as a function of current density for pulse duration ranging from 150 ns to 2 μs [Fig. 2(c)] exhibit a uniform depinning threshold current density $j_t \approx 3.9 \times 10^{11}$ A/m^2. The functional dependence of the velocity versus current density appears to be consistent with $\sqrt{j^2 - j_t^2}$, but the range of data (limited by the pulse amplitude) precludes any meaningful quantitive analysis. Pulses of 100 ns duration appear to yield slightly smaller displacements at all current densities and possibly a slightly higher j_t.

The location of the DW after pulsed B-field-stimulated injection and its displacement after application of a current pulse having current density above j_t are both affected by pinning potentials in the nanowire. The 90° bend functions like an engineered pinning center in the sense that the position of the injected DW is quite repeatable. The DW loca-

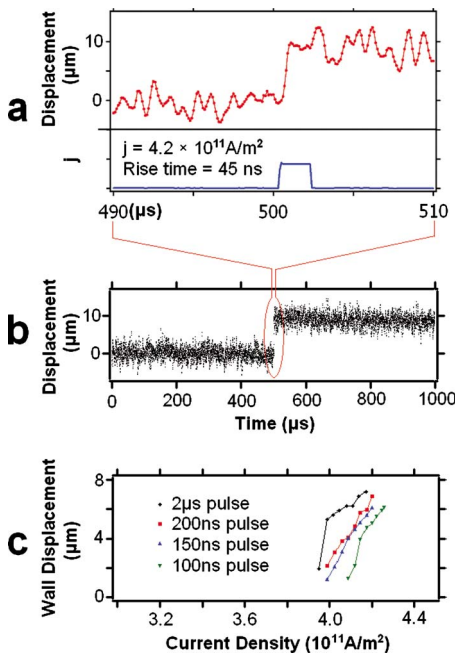

FIG. 2. (Color online) Panels (a) and (b): high temporal resolution (0.1 μs/sample) current-stimulated DW displacement produced by a 2-μs pulse. Panel (c): average wall displacement as a function of pulse duration and current density.

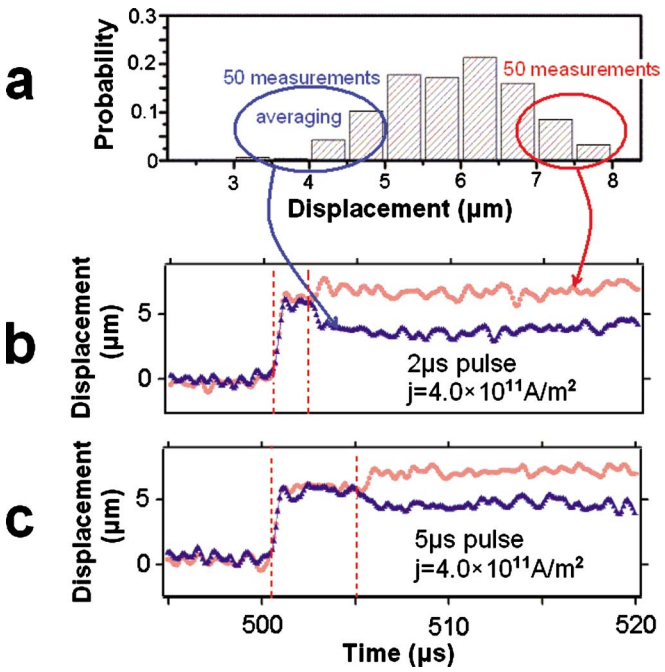

FIG. 3. (Color online) Panel (a): statistical distribution of DW displacements after 500 measurements for 2-μs pulses. Panels (b) and (c): typical signal-averaged time-resolved DW displacements for two current pulse widths selected to illustrate positive and negative displacement relaxation effects at the pulse termination, associated with upper (light, red dots) and lower (dark, blue triangles) regions of the distribution (refer to text).

tions within the polarimeter field of view prior to and after the current pulse are accurately measured (MOKE intensity); the DW displacements exhibit stochastic properties, which are discussed later. Averaged DW displacements scale with current density above j_t and appear to be independent of pulse duration for current pulse widths greater than 1 μs (refer to 2- and 5-μs displacements, Fig. 3), but exhibit some pulse-width dependence for shorter pulse widths [Fig. 2(c)].

Averaged DW displacements at $j=4\times10^{11}$ A/m^2 are $\Delta x\sim5$ μm [Fig. 2(c)] and occur on a time scale of 0.3 μs (or faster). This result allows a lower limit to be placed on the measured average velocity $v_{\min}\cong(5\ \mu\text{m})/(0.3\ \mu\text{s})\cong15$ m/s. This result is significantly higher than (average) DW velocities obtained in prior experiments.[11–13] The corresponding efficiency is also higher, $\epsilon\sim1$.

Figure 3 provides insight into the stochastic variations in current-driven DW displacements resulting from pulse excitation observed in prior experiments[11,12] and in the present experiment. The DW displacements are calculated by averaging 2000 0.1-μs samples prior to a specific ΔM transient [Fig. 2(a)] and 2000 samples after the transient, and subtracting these two averages. The Gaussian-like distribution [Fig. 3(a)] from a total of 500 measurements manifests the nondeterministic nature of pulse-current-driven DW displacements between pinning centers. Additional information about the dynamics can be obtained by signal averaging the magnetic transients selected from the upper and lower tails of the distribution [Fig. 3(a)]. Note that the noise for a single time-resolved displacement measurement at high temporal resolution (Fig. 2) is too large to resolve any details of the DW dynamics other than the prompt displacement initiated by the current step. Figures 3(b) and 3(c) display averages (50 measurements) of time-resolved DW displacements for 2-μs pulses [distribution, Fig. 3(a)] and 5-μs pulses (distribution not shown) in which the signal-averaged trace by triangles in each panel was obtained by selecting displacement records from the lower tail of the distribution and the trace defined by circles was obtained from corresponding displacement records from the upper tail. All time-resolved DW displacements exhibit the same behavior: (i) an abrupt initial displacement in the direction of electron transport triggered by the leading edge of $j(t)$ [this displacement increases with the increase of current density, Fig. 2(c)]; and (ii) a second abrupt smaller displacement in either direction at the termination of the pulse (the magnitude of this displacement also increases with current density). The initial displacement is nearly constant for pulses of variable width having the same current density, while both the amplitude and direction of the second displacement are random. The Gaussian-like distribution (upper panel, Fig. 3) is mainly due to the second displacement. Careful analysis of the averaged time-resolved DW position after the initial prompt displacement but prior to the pulse termination shows no evidence of a significant nonadiabatic contribution to DW displacement (which would manifest an additional systematic wall displacement in the direction of electron flow during the pulse). However, the jumps at the termination of $j(t)$ do suggest the presence of a (nonadiabatic) force of strength insufficient to overcome pinning.

Recent work by Thomas *et al.*[30] detected and characterized the oscillatory dependence of current-driven DW displacements on current pulse duration. In those experiments,

the bidirectional displacements were shown to result from the oscillation of the probability of dislodging a DW confined to a pinning center by a very short (ns duration) current pulse. Our experiments reveal a second mechanism that can produce bidirectional stochastic DW displacements stimulated at the termination of a (long duration) current pulse. LLG simulations of vortex-wall dynamics in Permalloy nanowire structure under high-field or current-drive conditions reveal motion in which the vortex core sweeps across the wire cross section perpendicular to the axis as it is driven along the wire in the direction of current or applied field.[21] Depinning and pinning of the vortex core occurs at the wire edges and the motion shows oscillation. We attribute the stochastic displacements of the wall at the termination of the current pulse to relaxation of the pinned vortex structure to a lower-energy pinned state when $j=0$ occurs.

In summary, this Rapid Communication presents time-resolved measurements of pulse-current-driven DW displacements in nanometer-scale Permalloy wires that manifest prompt motion wall velocities exceeding 15 m/s at $j=4\times10^{11}$ A/m^2 and spin-flip efficiencies $\epsilon\sim1$. These values are a factor of 10 higher than indicated in prior experiments, which have been interpreted to suggest that the adiabatic mechanism cannot explain pulse-driven DW dynamics. Most of the measured displacements occur within 0.3 μs of the leading edge of the pulse, and careful analysis of the wall position after the initial displacement (while current persists) shows no evidence of sustained motion that would occur if a significant nonadiabatic term contributed to wall displacement. The sample temperature was evaluated during the applied current pulses, and it was shown that the steady-state temperature remains significantly below the Curie temperature for Permalloy. These results suggest that the adiabatic spin-torque mechanism is a viable mechanism for the observed current-driven DW depinning and prompt displacements, and that spin-wave creation associated with depinning is not responsible for low spin-flip efficiencies determined from prior experiments. The DW displacement effects at the pulse termination suggest the presence of a nonadiabatic force that is too weak to overcome pinning.

The authors gratefully acknowledge useful discussions with G. S. D. Beach. This work was supported by the NSF-NIRT program Grant No. (DMR-0404252) and the Robert A. Welch Foundation Grant No. (F-1015). Instrumentation was developed with support from the NSF IMR Program Grant No. (DMR-0216726) and the Texas Coordinating Board Grant No. (ATP-0099). Device fabrication was carried out using facilities of the Center for Nano and Molecular Science and Technology at UT Austin.

[1] G. A. Prinz, Science **282**, 1660 (1998).
[2] S. A. Wolf *et al.*, Science **294**, 1488 (2001).
[3] D. A. Allwood *et al.*, Science **309**, 1688 (2005).
[4] G. Tatara and H. Kohno, Phys. Rev. Lett. **92**, 086601 (2004).
[5] Z. Li and S. Zhang, Phys. Rev. Lett. **92**, 207203 (2004).
[6] S. Zhang and Z. Li, Phys. Rev. Lett. **93**, 127204 (2004).
[7] Z. Li and S. Zhang, Phys. Rev. B **69**, 134416 (2004).
[8] Z. Li and S. Zhang, Phys. Rev. B **70**, 024417 (2004).
[9] A. Thiaville *et al.*, J. Appl. Phys. **95**, 7049 (2004).
[10] J. Xiao, A. Zangwill, and M. D. Stiles, Phys. Rev. B **73**, 054428 (2006).
[11] A. Yamaguchi, T. Ono, S. Nasu, K. Miyake, K. Mibu, and T. Shinjo, Phys. Rev. Lett. **92**, 077205 (2004).
[12] A. Yamaguchi *et al.*, Appl. Phys. Lett. **86**, 012511 (2005).
[13] M. Kläui, P. O. Jubert, R. Allenspach, A. Bischof, J. A. C. Bland, G. Faini, U. Rudiger, C. A. F. Vaz, L. Vila, and C. Vouille, Phys. Rev. Lett. **95**, 026601 (2005).
[14] S. H. Florez *et al.*, J. Appl. Phys. **97**, 10C705 (2005).
[15] C. K. Lim *et al.*, Appl. Phys. Lett. **84**, 2820 (2004).
[16] L. Berger, J. Appl. Phys. **49**, 2156 (1978).
[17] L. Berger, J. Appl. Phys. **55**, 1954 (1984).
[18] L. Berger, J. Appl. Phys. **71**, 2721 (1992).
[19] D. Atkinson *et al.*, Nat. Mater. **2**, 85 (2003).
[20] G. S. D. Beach *et al.*, Nat. Mater. **4**, 741 (2005).
[21] Y. Nakatani *et al.*, Nat. Mater. **2**, 521 (2003).
[22] M. D. Stiles *et al.* (unpublished).
[23] G. S. D. Beach, C. Knutson, C. Nistor, M. Tsoi, and J. L. Erskine, Phys. Rev. Lett. **97**, 057203 (2006).
[24] M. Hayashi, L. Thomas, Y. B. Bazaliy, C. Rettner, R. Moriya, X. Jiang, and S. S. P. Parkin, Phys. Rev. Lett. **96**, 197207 (2006).
[25] M. Klaui *et al.*, Appl. Phys. Lett. **85**, 5637 (2004).
[26] Y. Nakatani *et al.*, J. Magn. Magn. Mater. **290**, 750 (2005).
[27] C. Nistor *et al.*, Rev. Sci. Instrum. **77**, 103901 (2006).
[28] S. Yang and J. L. Erskine, Phys. Rev. B **72**, 064433 (2005).
[29] R. M. Bozorth, *Ferromagnetism* (Van Nostrand, Princeton, 1951).
[30] L. Thomas *et al.*, Nature (London) **443**, 197 (2006).